



43 frequency [ADA04]. Frequency hopping radar performance depends only slightly on the code used, given that  
 44 certain properties are met. This allows for a larger assortment of codes, making it even more difficult to intercept.  
 45 Time-frequency signal analysis includes the analysis and processing of signals

46 **2 a) Wigner-Ville Distribution (WVD)**

47 One of the most prominent time-frequency distribution members is the WVD. The WVD satisfies a great number  
 48 of desirable mathematical properties. It is always real-valued, it preserves time and frequency shifts, and it satisfies  
 49 marginal properties [AUG96], [QIA02]. The WVD is a transformation of a continuous time signal into the time-  
 50 frequency domain, and is computed by correlating the signal with a time and frequency translated version of  
 51 itself, making the WVD bilinear. In addition, the WVD exhibits the highest signal energy concentration in the  
 52 time-frequency plane [WIL06]. By using the WVD, an intercept receiver can come close to having a processing  
 53 gain near the LPI radar's matched filter processing gain [PAC09]. The WVD also contains cross term interference  
 54 between every pair of signal components, which may limit its applications [GUL07], [STE96], and which can make  
 55 the WVD time-frequency representation hard to interpret, especially if the components are numerous or close  
 56 to each other, and the more so in the presence of noise [BOA03]. This lack of readability can in turn translate  
 57 into decreased signal detection and parameter extraction metrics, potentially placing the intercept receiver signal  
 58 analyst in harm's way.

59 The WVD of a signal  $x(t)$  is given in equation (1) as:  $WVD(x(t)) = \int_{-\infty}^{\infty} x(t + \tau) x^*(t - \tau) e^{-j2\pi f\tau} d\tau$  \*  
 60  $WVD(x(t)) = \int_{-\infty}^{\infty} x(t + \tau) x^*(t - \tau) e^{-j2\pi f\tau} d\tau$  \*  
 61 or equivalently in equation (2) as:  $WVD(x(t)) = \int_{-\infty}^{\infty} x(t + \tau) x^*(t - \tau) e^{-j2\pi f\tau} d\tau$  \*  
 62  $WVD(x(t)) = \int_{-\infty}^{\infty} x(t + \tau) x^*(t - \tau) e^{-j2\pi f\tau} d\tau$  \*

63 **b) Reassigned Smooth Pseudo Wigner-Ville Distribution (RSPWVD)**

64 The original idea of reassignment was introduced in an attempt to improve the Spectrogram [OZD03]. As  
 65 with any other bilinear energy distribution, the Spectrogram is faced with the trade-off between the reducing the  
 66 misleading interference terms and sharpening the localization of the signal components.

67 We can define the Spectrogram as a twodimensional convolution of the WVD of the signal by the WVD of the  
 68 analysis window, as in equation (3):  $SG(x(t), w(t)) = \int_{-\infty}^{\infty} WVD(x(t)) WVD(w(t)) e^{-j2\pi f\tau} d\tau$  \*  
 69  $SG(x(t), w(t)) = \int_{-\infty}^{\infty} WVD(x(t)) WVD(w(t)) e^{-j2\pi f\tau} d\tau$  \*

70 Therefore, the distribution reduces the interference terms of the signal's WVD, but at the expense of time  
 71 and frequency localization. But a closer look at equation (3) shows that  $(t, f)$  point, inside which a weighted average  
 72 delimits a time-frequency domain at the vicinity of the  $(t, f)$  point, inside which a weighted average  
 73 of the signal's WVD values is performed. The key point of the reassignment principle is that these values really  
 74 have no reason to be symmetrically distributed around  $(t, f)$ , the geometrical center of this domain.  
 75 Their average should not be assigned at this point, but rather at the center of gravity of this domain, which is  
 76 more representative of the local energy distribution of the signal [AUG94]. Using a mechanical analogy, the local  
 77 energy distribution  $WVD(x(t))$  (as a function of  $(t, f)$ ) can be  
 78 considered as a mass distribution, and it is much more accurate to assign the total mass (i.e. the Spectrogram  
 79 value) to the center of gravity of the domain rather than to its geometrical center. Another way to look at it is  
 80 this: the total mass of an object is assigned to its geometrical center, an arbitrary point which, except in the very  
 81 specific case of a homogeneous distribution, has no reason to suit the actual distribution. A more meaningful  
 82 choice is to assign the total mass of an object, as well as the Spectrogram value, to the center of gravity of their  
 83 respective distribution [BOA03]. This is exactly how the reassignment method proceeds: it moves each value of  
 84 the Spectrogram computed at any point  $(t, f)$  to another point  $(t', f')$  which is the center  
 85 of gravity of the signal energy distribution around  $(t, f)$  (see equations (??) and (??)) [LIX08]:  $SG(x(t), w(t)) = \int_{-\infty}^{\infty} WVD(x(t)) WVD(w(t)) e^{-j2\pi f\tau} d\tau$  \*  
 86  $SG(x(t), w(t)) = \int_{-\infty}^{\infty} WVD(x(t)) WVD(w(t)) e^{-j2\pi f\tau} d\tau$  \*  
 87  $SG(x(t), w(t)) = \int_{-\infty}^{\infty} WVD(x(t)) WVD(w(t)) e^{-j2\pi f\tau} d\tau$  \*

88 leading to a reassigned Spectrogram (equation (??)), whose value at any point  $(t, f)$  is the  
 89 sum of all the Spectrogram values reassigned to this point:  $SG(x(t), w(t)) = \int_{-\infty}^{\infty} WVD(x(t)) WVD(w(t)) e^{-j2\pi f\tau} d\tau$  \*  
 90  $SG(x(t), w(t)) = \int_{-\infty}^{\infty} WVD(x(t)) WVD(w(t)) e^{-j2\pi f\tau} d\tau$  \*  
 91  $SG(x(t), w(t)) = \int_{-\infty}^{\infty} WVD(x(t)) WVD(w(t)) e^{-j2\pi f\tau} d\tau$  \*

92 An interesting property of this new distribution is that it also uses the phase information of the STFT, and  
 93 not just its squared modulus, as in the Spectrogram. It uses this information from the phase spectrum in order  
 94 to sharpen the amplitude estimates in both time and frequency. This can be seen from the following expressions  
 95 of the reassignment operators: (??). This leads to an efficient implementation for the Reassigned Spectrogram  
 96 without explicitly computing the partial derivatives of phase. The Reassigned Spectrogram may thus be computed  
 97 by using 3 STFTs, each having a different window (the window function  $h$ ; the same window with a weighted time  
 98 ramp  $t^*h$ ; and, the derivative of the window function  $h$  with respect to time ( $dh/dt$ )). Reassigned Spectrograms  
 99 are therefore very computationally efficient to implement.  $SG(x(t), w(t)) = \int_{-\infty}^{\infty} WVD(x(t)) WVD(w(t)) e^{-j2\pi f\tau} d\tau$  \*

100 Since time-frequency reassignment is not a bilinear operation, it does not permit a stable reconstruction of  
 101 the signal. In addition, once the phase information has been used to reassign the amplitude coefficients, it is no  
 102 longer available for use in reconstruction.

103 For this reason, the reassignment method has received limited attention from engineers, and its greatest  
 104 potential seems to be where reconstruction is not necessary, that is, where signal analysis is an end unto itself.

---

105 One of the most important properties of the reassignment method is that the application of the reassignment  
106 process to any distribution of Cohen's class, theoretically yields perfectly localized distributions for chirp signals,  
107 frequency tones, and impulses. This is one of the reasons that the reassignment method was chosen for this paper  
108 as a signal processing technique for analyzing LPI radar waveforms such as the frequency hopping waveforms  
109 (which can be viewed as multiple tones).

110 In order to resolve the classical time-frequency analysis deficiency of cross-term interference, a method needs  
111 to be used which reduces cross-terms, which the reassignment method does.

112 The reassignment principle for the Spectrogram allows for a straight-forward extension of its use for other  
113 distributions as well [HIP00], including the WVD. If we consider the general expression of a distribution of the  
114 Cohen's class as a two-dimensional convolution of the WVD, as in equation ( ??1

## 115 3 II. Methodology

116 The methodologies detailed in this section describe the processes involved in obtaining and comparing metrics  
117 between the classical time-frequency analysis techniques of the Wigner-Ville Distribution and the Reassigned  
118 Smoothed Pseudo Wigner-Ville Distribution for the detection and characterization of low probability of intercept  
119 frequency hopping radar signals.

120 The tools used for this testing were: MATLAB (version 8.3), Signal Processing Toolbox (version 6.21), and  
121 Time-Frequency Toolbox (version 1.0). All testing was accomplished on a desktop computer.

122 Testing was performed for the 4-component frequency hopping waveform. Waveform parameters were chosen  
123 for academic validation of signal processing techniques. Due to computer processing resources they were not  
124 meant to represent real-world values. The number of samples for each test was chosen to be 512, which seemed to  
125 be the optimum size for the desktop computer. Testing was performed at three different SNR levels: 10dB, 0dB,  
126 and the lowest SNR at which the signal could be detected. The noise added was white Gaussian noise, which  
127 best reflects the thermal noise present in the IF section of an intercept receiver [PAC09]. Kaiser windowing was  
128 used, when windowing was applicable. 100 runs were performed for each test, for statistical purposes. The plots  
129 included in this paper were done at a threshold of The frequency hopping (prevalent in the LPI arena [AMS09]) 4-  
130 component signal had parameters of: sampling frequency=5KHz; carrier frequencies=1KHz, 1.75KHz, 0.75KHz,  
131 1.25KHz; modulation bandwidth=1KHz; modulation period=.025sec.

132 After each particular run of each test, metrics were extracted from the time-frequency representation.

133 The different metrics extracted were as follows:

134 1) Relative Processing Time: The relative processing time for each time-frequency representation.

135 2) Percent Detection: Percent of time signal was detected. Signal was declared a detection if any portion of  
136 each of the 4 signal components exceeded a set threshold (a certain percentage of the maximum intensity of the  
137 time-frequency representation). Threshold percentages were determined based on visual detections of low SNR  
138 signals (lowest SNR at which the signal could be visually detected in the timefrequency representation). Based  
139 on the above methodology, thresholds were assigned as follows for the signal processing techniques used for this  
140 paper: WVD (50%); RSPWVD (50%).

141 For percent detection determination, these threshold values were included in the time-frequency plot algorithms  
142 so that the thresholds could be applied automatically during the plotting process. From the threshold plot, the  
143 signal was declared a detection if any portion of each of the signal components was visible (see Figure 1). The  
144 threshold percentage was determined based on manual measurement of the modulation bandwidth of the signal  
145 in the time-frequency representation. This was accomplished for ten test runs of each time-frequency analysis  
146 tool (WVD and RSPWVD). During each manual measurement, the max intensity of the high and low measuring  
147 points was recorded. The average of the max intensity values for these test runs was 20%. This was adopted as  
148 the threshold value, and is representative of what is obtained when performing manual measurements. This 20%  
149 threshold was also adapted for determining the modulation period and the time-frequency localization (both are  
150 described below).

151 For modulation bandwidth determination, the 20% threshold value was included in the time-frequency plot  
152 algorithms so that the threshold could be applied automatically during the plotting process. From the threshold  
153 plot, the modulation bandwidth was manually measured (see Figure 3). For lowest detectable SNR determination,  
154 these threshold values (WVD (50%); RSPWVD (50%)) were included in the time-frequency plot algorithms so  
155 that the thresholds could be applied automatically during the plotting process. From the threshold plot, the  
156 signal was declared a detection if any portion of each of the 4 signal components was visible. The lowest SNR  
157 level for which the signal was declared a detection is the lowest detectable SNR.

158 The data from all 100 runs for each test was used to produce the actual, error, and percent error for each of  
159 these metrics listed above.

160 The metrics from the WVD were then compared to the metrics from the RSPWVD. By and large, the  
161 RSPWVD outperformed the WVD, as will be shown in the results section.

## 162 4 III. Results

163 Table 1 presents the overall test metrics for the two classical time-frequency analysis techniques used in this  
164 testing (WVD versus RSPWVD). 1, the RSPWVD outperformed the WVD in average percent error: carrier

165 frequency (0.12% vs. 0.21%), modulation bandwidth (4.72% vs. 6.07%), modulation period (6.05% vs. 16.51%),  
 166 and timefrequency localization (y-direction) (1.28% vs. 2.14%); and in average: percent detection (94.1% vs.  
 167 90.2%), lowest detectable SNR (-3.0dB vs. -2.0dB) and average relative processing time (0.023s vs. 0.682s).

168 Figure 6 shows comparative plots of the WVD vs. the RSPWVD (4-component frequency hopping) at SNRs  
 169 of 10dB (top), 0dB (middle), and lowest detectable SNR (-2.0dB for WVD and -3.0dB for RSPWVD) (bottom).

## 170 5 Global Journal of Researches in Engineering

### 171 6 IV. Discussion

172 This section will elaborate on the results from the previous section.

173 From Table 1, the RSPWVD outperformed the WVD in average percent error: carrier frequency (0.12% vs.  
 174 0.21%), modulation bandwidth (4.72% vs. 6.07%), modulation period (6.05% vs. 16.51%), and timefrequency  
 175 localization (y-direction) (1.28% vs. 2.14%); and in average: percent detection (94.1% vs. 90.2%), lowest  
 176 detectable SNR (-3.0dB vs. -2.0dB) and average relative processing time (0.023s vs. 0.682s). These results are  
 177 the result of the RSPWVD signal being a more localized signal than the WVD signal, along with the fact that  
 178 the WVD signal has cross-term interference, which the RSPWVD doesn't have.

179 The RSPWVD might be used in a scenario where you need good signal localization in a fairly low SNR  
 180 environment, in a short amount of time. The RSPWVD would be preferred over the WVD in virtually every  
 181 scenario, based on the metrics obtained. Digital intercept receivers, whose main job is to detect and extract  
 182 parameters from low probability of intercept radar signals, are currently moving away from Fourier-based analysis  
 183 and moving towards classical time-frequency analysis techniques, such as the WVD and the RSPWVD, for the  
 184 purpose of analyzing low probability of intercept radar signals. Based on the research performed for this paper  
 185 (the novel direct comparison of the WVD versus the RSPWVD for the signal analysis of low probability of  
 186 intercept frequency hopping radar signals) it was shown that the RSPWVD by and large outperformed the WVD  
 187 for analyzing these low probability of intercept radar signals -for reasons brought out in the discussion section  
 188 above. More accurate characterization metrics may well equate to saved equipment and lives.

189 Future plans include analysis of an additional low probability of intercept radar waveform 8-component  
 frequency Hopper, again using the WVD and the RSPWVD as time-frequency analysis techniques.

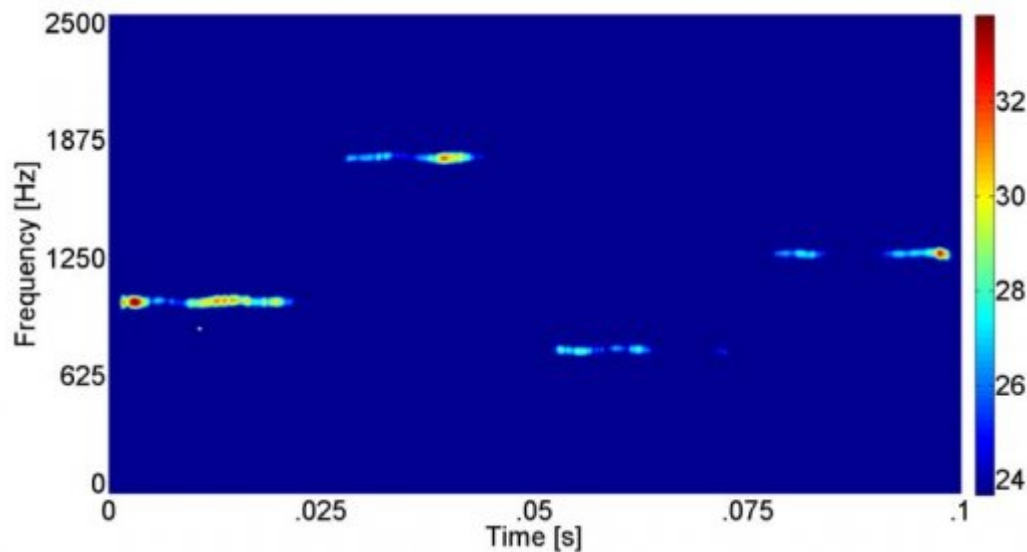


Figure 1:

190 1  
 191

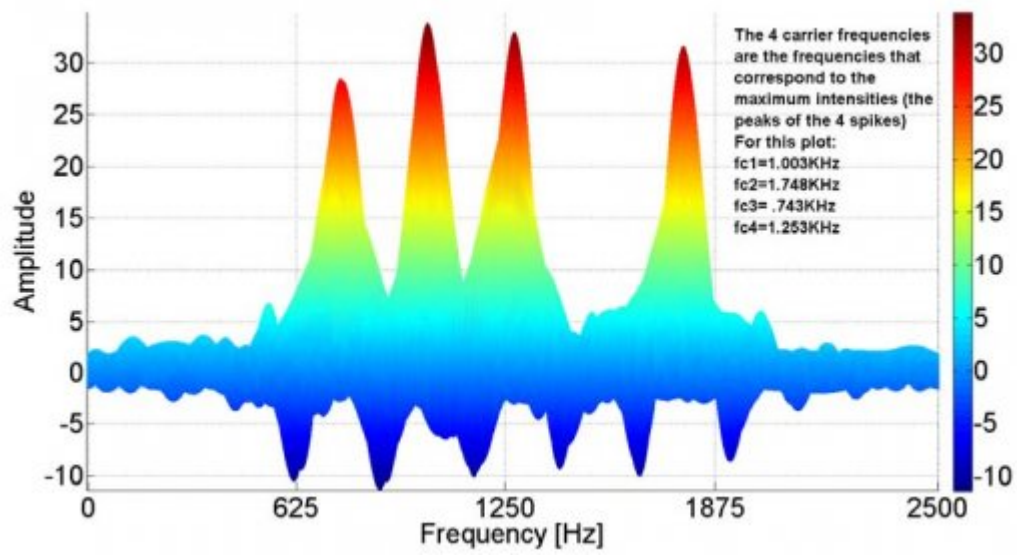


Figure 2:

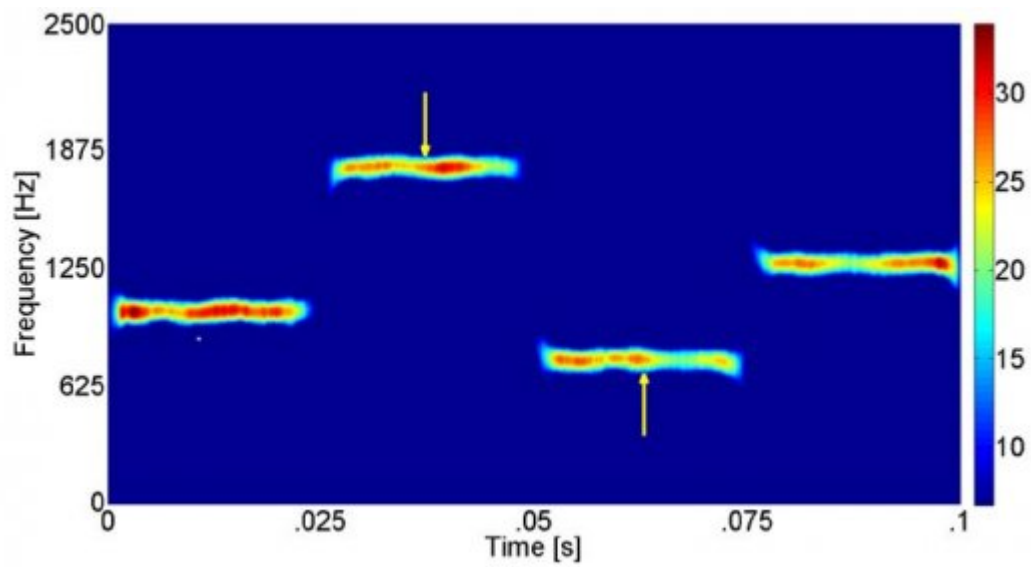


Figure 3:

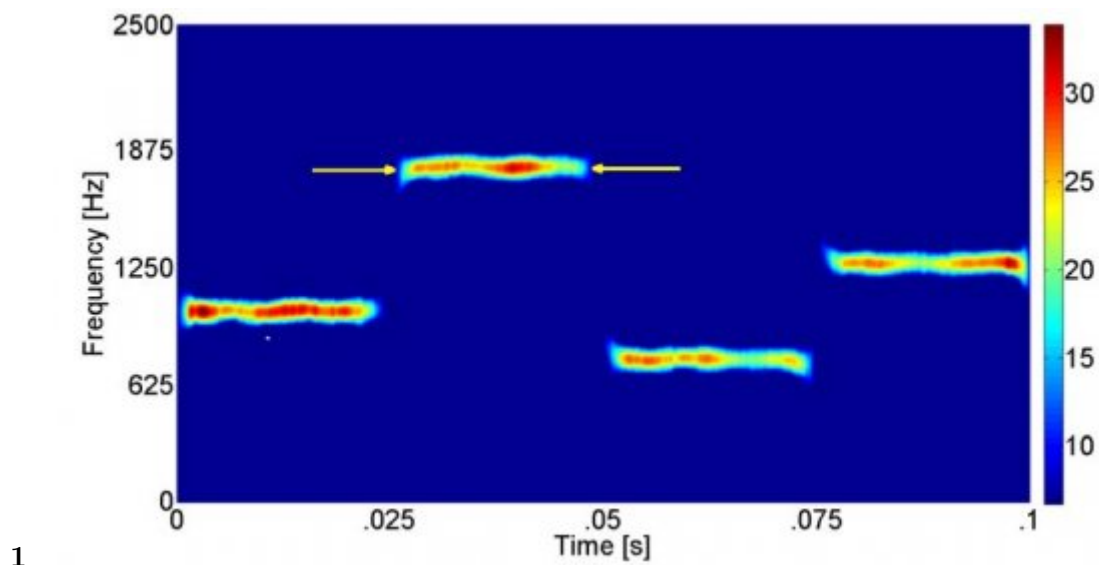


Figure 4: Figure 1 :

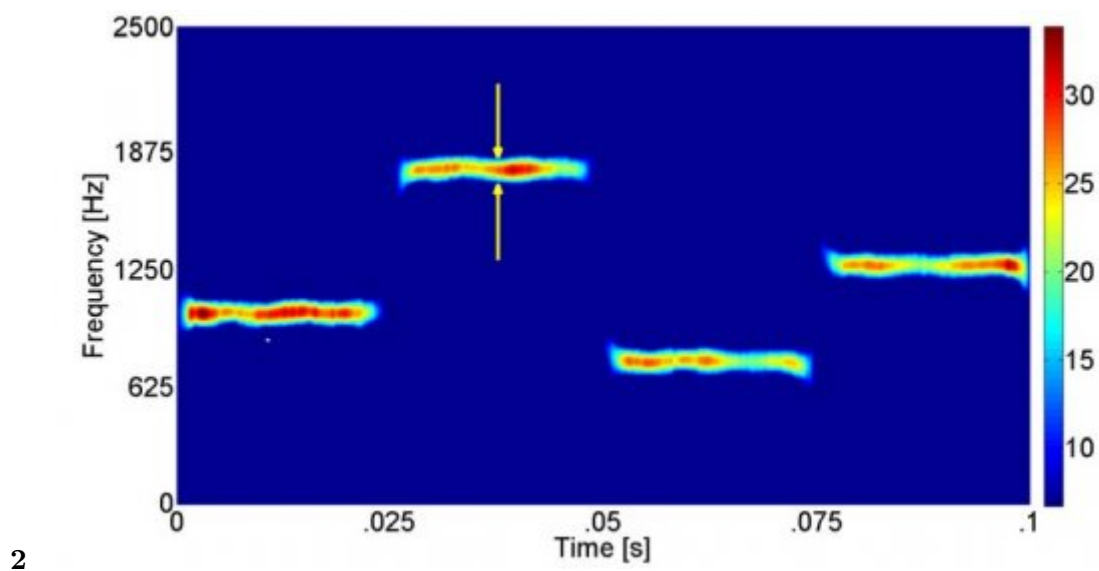
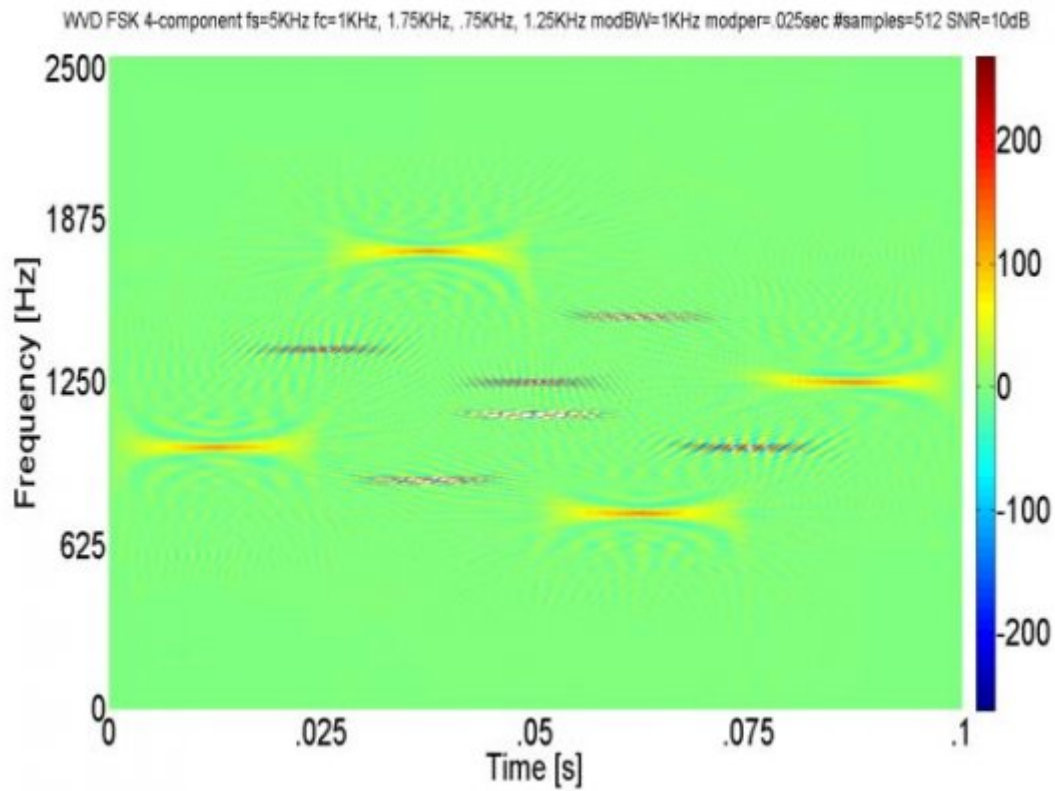
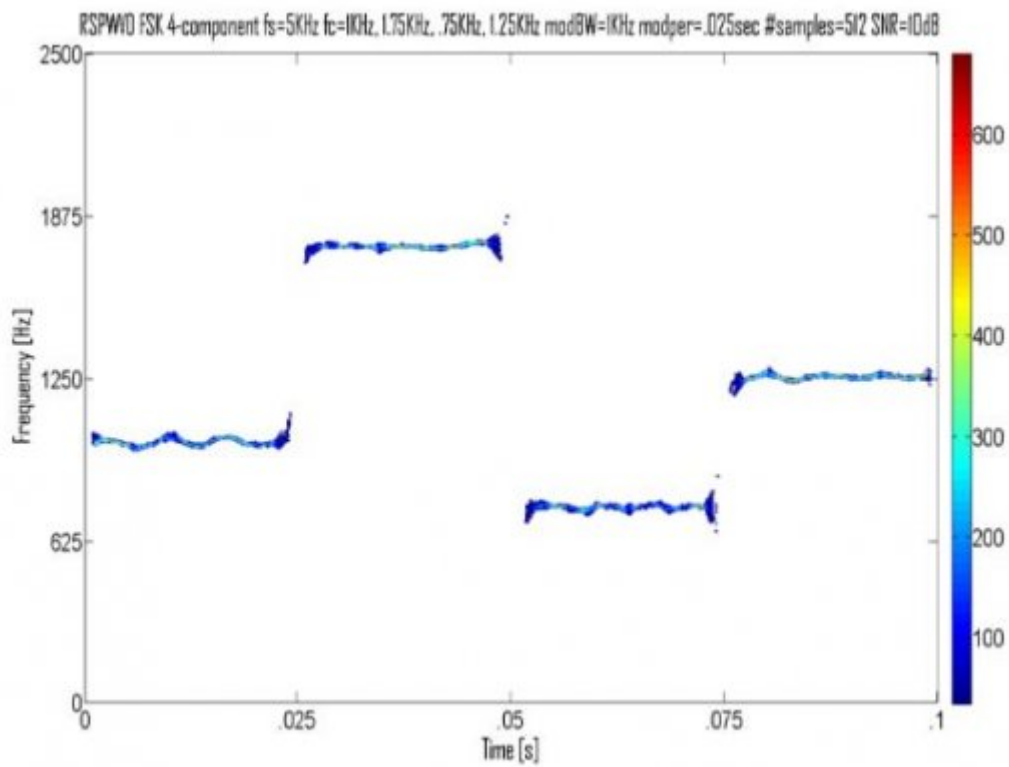


Figure 5: Figure 2 :



3

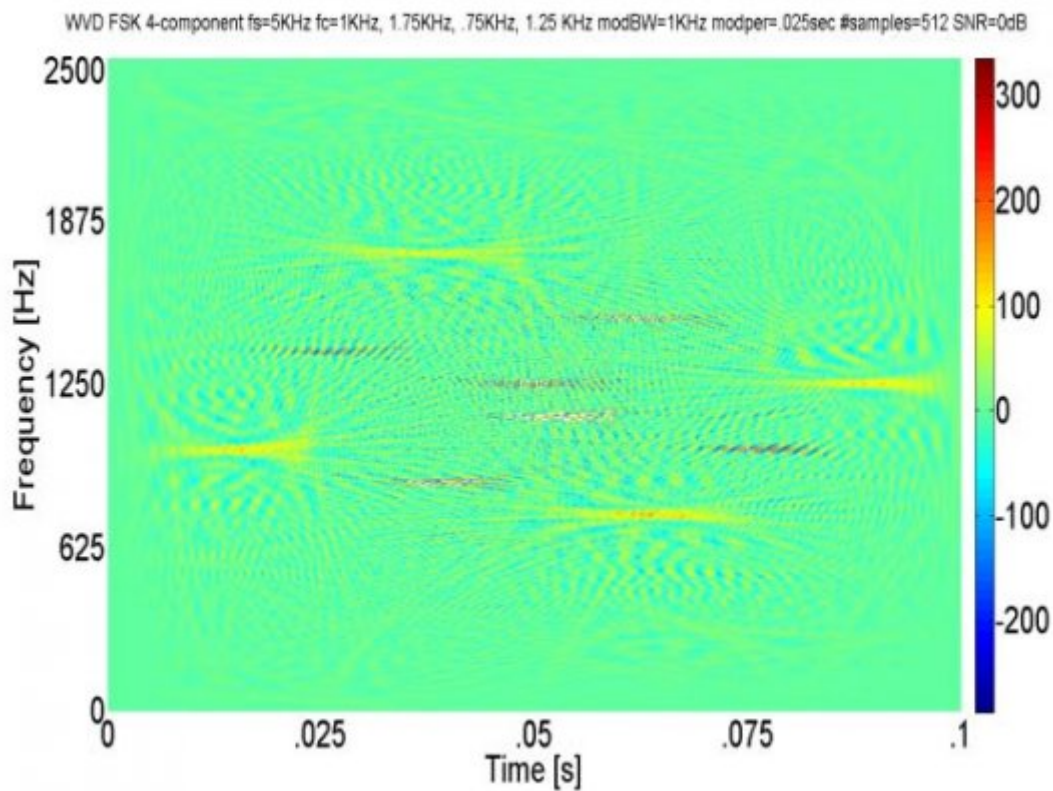
Figure 6: Figure 3 :FA



4

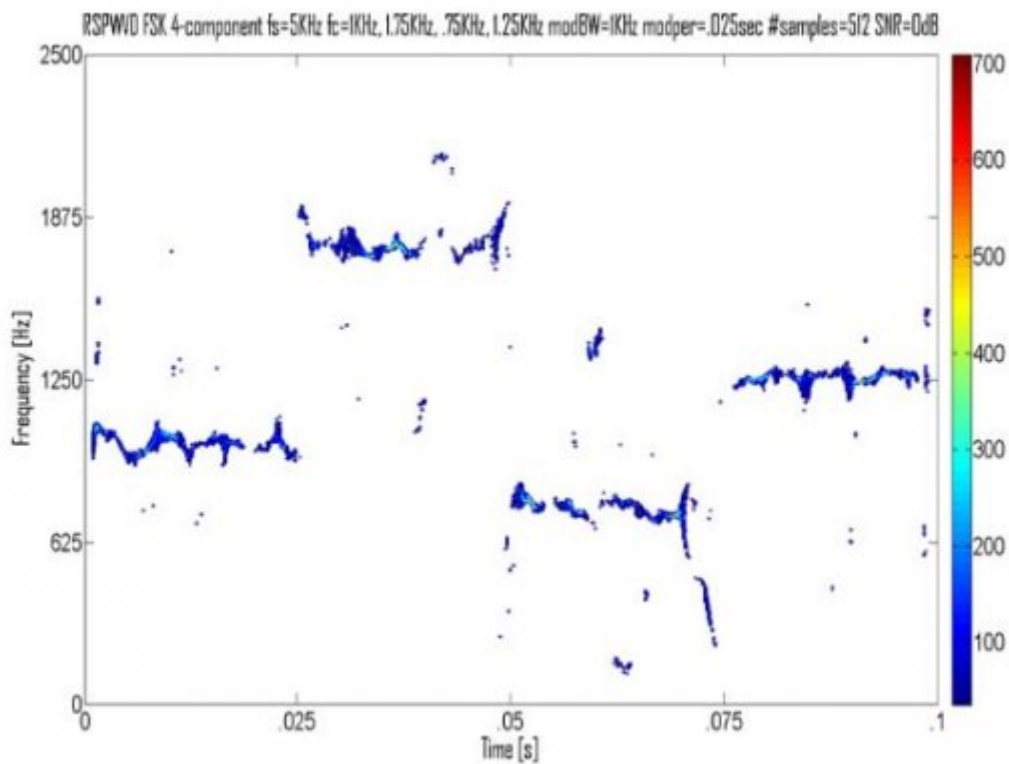
Figure 7: Figure 4 :





5

Figure 8: Figure 5 :



6

Figure 9: Figure 6 :



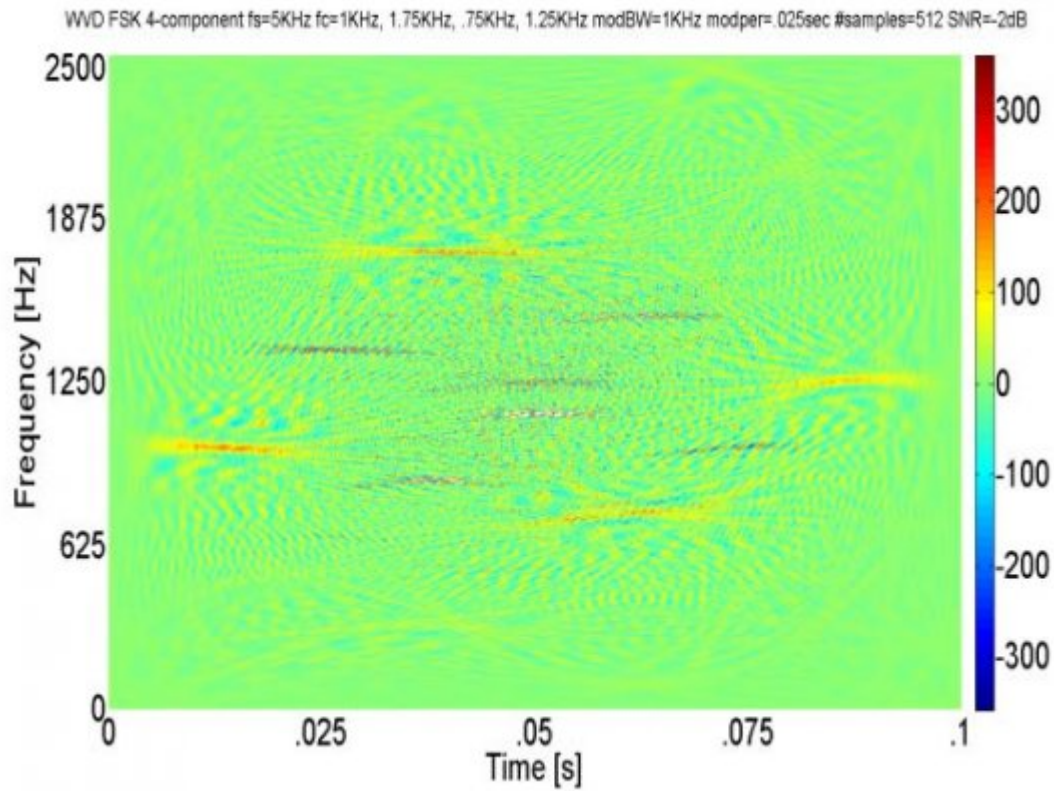


Figure 10:

1

carrier frequency, modulation bandwidth, modulation period; average: time-frequency localization-y (as percent of y-axis), percent detection, lowest detectable snr, relative processing time) for the two classical time-frequency analysis techniques (WVD versus RSPWVD)

Parameters	WVD	RSPWVD
Carrier Frequency	0.21%	0.12%
Modulation Bandwidth	6.07%	4.72%
Modulation Period	16.51%	6.05%
Time-Frequency Localization-Y	2.14%	1.28%
Percent Detection	90.2%	94.1%
Lowest Detectable SNR	-2.0dB	-3.0dB
Relative Processing Time	0.682s	0.023s

Figure 11: Table 1 :

Year 2022  
7  
Volume Xx XII Issue III V ersion I  
( )  
© 2022 Global Journals

Figure 12: F

- 
- 192 [Papandreou] , A Papandreou . Boudreaux-Bartels.
- 193 [Anjaneyulu et al. (2009)] ‘A Novel Method for Recognition of Modulation Code of LPI Radar Signals’. L  
 194 Anjaneyulu , N Murthy , N Sarma . *International Journal of Recent Trends in Engineering* May 2009. 1  
 195 (3) p. .
- 196 [Stephens (1996)] ‘Advances in Signal Processing Technology for Electronic Warfare’. J Stephens . *IEEE AES*  
 197 *Systems Magazine* November 1996. p. .
- 198 [Wei et al. (2003)] ‘Analysis of Multicomponent LFM Signals Using Time-Frequency and The Gray-Scale Inverse  
 199 Hough Transform’. G Wei , S Wu , E Mao . *IEEE Workshop on Statistical Signal Processing* September 28  
 200 -October 1, 2003. p. .
- 201 [Gulum ()] *Autonomous Non-Linear Classifications of LPI Radar Signal Modulations. Thesis, Naval Postgraduate*  
 202 *School, T Gulum . 2007. Monterey, CA.*
- 203 [Pace ()] *Detecting and Classifying Low Probability of Intercept Radar*, P Pace . 2009. Norwood, MA: Artech  
 204 House.
- 205 [Kay ()] ‘Detection and Estimation of Generalized Chirps Using Time-Frequency Representations’. G F Kay , S  
 206 . *Conference Record of the Twenty-Eighth Asilomar Conference on Signals, Systems and Computers*, 1994.  
 207 1994. p. .
- 208 [Upperman (2008)] *ELINT Signal Processing Using Choi-Williams Distribution on Reconfigurable Computers for*  
 209 *Detection and Classification of LPI Emitters. Thesis, Naval Postgraduate School, T Upperman . March 2008.*  
 210 *Monterey, CA.*
- 211 [Adamy ()] *EW 102: A Second Course in Electronic Warfare*, D Adamy . 2004. Norwood, MA: Artech House.
- 212 [Gulum et al. (2008)] ‘Extraction of Polyphase Radar Modulation Parameters Using a Wigner-Ville Distribution-  
 213 Radon Transform’. T Gulum , P Pace , R Cristi . *IEEE International Conference on Acoustics, Speech, and*  
 214 *Signal Processing*, (Las Vegas, NV) April 2008.
- 215 [Rangayyan and Krishnan ()] ‘Feature Identification in the Time-Frequency Plane by Using the Hough-Radon  
 216 Transform’. R Rangayyan , S Krishnan . *Pattern Recognition* 2001. 34 p. .
- 217 [Anjaneyulu et al. (2009)] *Identification of LPI Radar Signal Modulation using Bi-coherence Analysis and*  
 218 *Artificial Neural Networks Techniques*, L Anjaneyulu , N Murthy , N ; Sarma , Iit Guwahati . 2009. January  
 219 16-18, 2009. p. .
- 220 [Choi and Williams (1989)] ‘Improved Time-Frequency Representation of Multicomponent Signals Using Exponential  
 221 Kernels’. H Choi , W Williams . *IEEE Transactions on Acoustics, Speech, and Signal Processing* June  
 222 1989. 37 p. .
- 223 [Qian ()] *Introduction To Time-Frequency and Wavelet Transforms*, S Qian . 2002. Upper River, NJ: Prentice  
 224 Hall.
- 225 [Li and Bi ()] X Li , G Bi . *A New Reassigned Time-Frequency Representation. 16 th European Signal Processing*  
 226 *Conference*, (Lausanne, Switzerland) August 25-29, 2008. p. .
- 227 [Hlawatsch and Boudreaux-Bartels (1992)] ‘Linear and Quadratic Time-Frequency Signal Representations’. F  
 228 Hlawatsch , G F Boudreaux-Bartels . *IEEE Signal Processing Mag* April 1992. 9 (2) p. .
- 229 [Polyphase and Waveforms ()] Lpi Polyphase , Waveforms . *Proceedings of ICASSP*, (ICASSP Orlando, FL) 2002.  
 230 p. .
- 231 [Li and Xiao (2003)] ‘Recursive Filtering Radon-Ambiguity Transform Algorithm for Detecting Multi-LFM  
 232 Signals’. Y Li , X Xiao . *Journal of Electronics (China)* May 2003. 20 (3) p. .
- 233 [Han et al. (2000)] ‘Target Position Extraction Based on Instantaneous Frequency Estimation in a Fixed-Reticle  
 234 Seeker’. S Han , H Hong , D Seo , J Choi . *Opt. Eng* September 2000. 39 p. .
- 235 [Boashash ()] *Time Frequency Signal Analysis and Processing: A Comprehensive Reference*, B Boashash . 2003.  
 236 Oxford, England: Elsevier.
- 237 [Ozdemir (2003)] *Time-Frequency Component Analyzer. Dissertation*, A Ozdemir . Sept. 2003. Ankara, Turkey.  
 238 Bilkent University
- 239 [Auger et al. ()] *Time-Frequency Toolbox Users Manual*, F Auger , P Flandrin , P Goncalves , O Lemoine . 1996.  
 240 Centre National de la Recherche Scientifique and Rice University
- 241 [Milne and Pace] *Wigner Distribution Detection and Analysis of FMCW and P-4*, P Milne , P Pace .